Synthesis and Characterization of Crosslinked Chitosan Immobilized on Bentonite and Its Grafted Products with Polyaniline

ARTICLE *in* JOURNAL OF APPLIED POLYMER SCIENCE · NOVEMBER 2014

Impact Factor: 1.77 · DOI: 10.1002/app.41078

5 AUTHORS, INCLUDING:

Hassan Hefni Hassan Hefni
Egyptian Petroleum Research Institute
11 PUBLICATIONS **49** CITATIONS

JOURNAL OF Applied Polymer SCIENCE

Synthesis and Characterization of Crosslinked Chitosan Immobilized on Bentonite and Its Grafted Products with Polyaniline

Fawzia I. El-Dib, Mohammed H. M. Hussein, Hassan H. H. Hefni, Ghada Eshaq, Ahmed E. ElMetwally
Department of Petrochemicals, Egyptian Petroleum Research Institute, Nasr City, Cairo 11727, Egypt
Correspondence to: G. Eshaq (E-mail: ghadaamer2002@yahoo.com).

ABSTRACT: Chitosan immobilized bentonite (CIB) namely chitosan-coated bentonite (5% chitosan content) was synthesized in 2% acetic acid solution, followed by crosslinking, using epichlorohydrien (ECH). The so-obtained crosslinked chitosan immobilized on bentonite (CIB-ECH) and CIB composites were grafted with polyaniline (PANI) through oxidative-radical copolymerization using ammonium peroxydisulfate in acidic medium to produce PANI-grafted crosslinked chitosan immobilized on bentonite (PANI-*g*-CIB-ECH) and PANI-grafted-chitosan immobilized on bentonite (PANI-*g*-CIB) composites, respectively. The resultant composites were characterized by using X-ray diffraction (XRD), thermo gravimetric analysis/differential scanning calorimetry, scanning electron microscopy, Fourier transform infrared (FTIR), and electrical conductivity. XRD and FTIR analyses indicate that chitosan was not intercalated into the silicate layer. Also the electrical conductivity elucidates that the grafted composites fall in the range required for the application as electrostatic dissipation. © 2014 Wiley Periodicals, Inc. J. Appl. Polym. Sci. **2014**, *131*, 41078.

KEYWORDS: conducting polymers; crosslinking; grafting

Received 7 April 2014; accepted 27 May 2014
DOI: 10.1002/app.41078

INTRODUCTION

Chitosan, a polycationic polymer and waste product from seafood processing industry, is an abundant natural resource that has, as yet, not been fully utilized. The advantage of this natural biopolymer includes availability, low cost, nontoxic, high biocompatibility, biodegradability, and ease chemical modification. Chitosan can be used for example in water treatment, pharmaceutical products, agriculture, and membrane formation.[1] It is well known to be an excellent adsorption because it contains hydroxyl (—OH) and amino ($—NH_2$) groups that serve as metal binding sites.[2] However, chitosan has a low surface area with weak chemical and mechanical properties. Therefore, physical and chemical properties are necessary to overcome these limitations.

Physical modification allows the expansion of the chitosan polymer chain, which decrease its crystallinity and causes the accessibility of its binding sites. Providing a proper and inexpensive material to be used as an immobilization support for chitosan would assist in lowering the quantity of chitosan needed in the treatment process.[3,4] Among the adsorbent, the chitosan immobilizing in clay is one of the cheapest materials and has high efficiency in removing heavy metals.[3,5,6] On the other hand, chemical modification such as sulfonation, grafting, blending, carboxylation, and crosslinking are utilized to improve mechanical strength, chemical stability, and hydrophilicity, to prevent dissolution in dilute acidic medium, and to enhance its selectivity for metal adsorption. Among the chemical methods, crosslinking has received much attention due to its simple procedure and ability to form macromolecular structure for a variety of applications.[7] The chitosan composites crosslinked with epichlorohydrin (ECH) were able to improve the chitosan performance as an adsorbent.[8] A crosslinking agent can stabilize chitosan in acid solution so that chitosan becomes insoluble.

Conducting polyanilines (PANIs) have increasing scientific and technological interest in the synthesis of a broad variety of promising new materials due to their unique electrical, optical, and optoelectrical properties as well as the ease of preparation and environmental stability.[9,10] Clay\polymer nanocomposites offer tremendous improvement in a wide range of physical properties. This method is currently emphasized commercially and has received great attention in recent years.[11] The formation of PANI composites with inorganic materials provides new synergistic properties that cannot be attained from individual materials.[12] From the industrial point of view, the fabrication of thermally processable conducting polymer would be preferable. Composite formation improves the mechanical properties of PAN1 and the electrical conductivity can be tailored for a given application. They have attractive mechanical and other properties of the inorganic materials. For the application as electrostatic dissipation (ESD), the conductivity levels required are approximately in the range of $10^{-5}—10^{-9}$ S cm^{-1}.

Grafting of chitosan is a common way to improve its properties such as increasing chelation[13] or complexation properties[14] or enhancing adsorption properties.[15] In the present work, chitosan immobilized on bentonite (CIB) and crosslinking chitosan immobilized on bentonite (CIB-ECH) were synthesized. PANI was grafted onto both CIB and CIB-ECH in order to synthesize low cost tailor-made composites having good thermal stability and electrical conductivity falls in the range required for the applications as ESD. Characterization of the composites has been carried out using X-ray diffraction (XRD), thermo gravimetric analysis (TGA)/differential scanning calorimetry (DSC), Fourier transform infrared (FTIR), scanning electron microscopy (SEM), and conductivity.

EXPERIMENTAL

Materials and Equipments

Chitosan flakes with 82% degree of deacetylation and 110 kDa of molecular weight was prepared according to the method in the literature.[16] Bentonite from El-Tih region (East Abu-Zenima, Sinai Peninsula, Egypt) was ground, sieved to particle diameter less than 125 μm, and then subjected to activation by treatment via 2% hydrochloric acid solution for 6 h at 104°C in order to remove carbonates and soluble salts.[17] The clay was washed repeatedly with distilled water till free from chloride then dried at 120°C for 2 h.

ECH as crosslinking agent with 99% purity was produced from Sigma Aldrich (Germany), hydrochloric acid (37% fuming) and sodium hydroxide were obtained from Merck Germany. All reagents used were analytical grade. Deionized (DI) water was used to prepare all reagent solutions. Aniline, ammonium peroxydisulfate, and acetic acid (Fluka) were used as received. XRD analysis was performed using a Bruker D8 Series with a slow scan at 0.3° s^{-1} in 2θ range of 2°–25°. The thermal properties, TGA, and DSC were performed by STA 625-PL Thermal Science. A FTIR spectra recorded between 400 and 4000 cm^{-1} with a 4 cm^{-1} resolution from KBr pellets on a Perkin Elmer spectra BX FTIR system (Beaconsfield Beuckinghamshire, HP91QA, England). The direct current electrical conductivity of the composites was measured by the standard four point probe method using PCI-DAS6014 for a current source, voltmeter, and temperature controller. Dry powder samples were made into pellets using a steel die of 13 mm diameter in hydraulic press under a pressure of 700 MPa. SEM was employed to study the type of the surface morphology of composites. A Cambridge S-360 SEM was used for this purpose.

Methods

Preparation of Chitosan Immobilized on Bentonite. A 5.0 g of chitosan were dissolved in 300 mL 0f 5% (vol/vol) HCl under vigorous stirring for 2 h. After chitosan dissolution, 100 g of clay (bentonite) was added into the solution and stirred for 3 h at 25°C. The chitosan clay solution neutralized with 1*N* NaOH (pH 13) that was added in a dropwise method until the chitosan has precipitated.[18] The chitosan–bentonite beads was filtered and washed with DI water to remove excess NaOH. The CIB was dried in the oven at 65°C for 24 h. After grinding the particles, called CIB [Scheme 1(A)], they were passed through ASTM sieve size no. 35 and no. 45. CIB with bead size range of 0.35–0.50 mm was utilized.

Preparation of Crosslinked Chitosan Immobilized on Bentonite. An equimolar 1 : 1 of chitosan to ECH was prepared. About 1.162 mL of ECH was added into the chitosan–bentonite solution. The CIB solution was stirred continuously at 55°C for 2 h. The crosslinked CIB (Scheme 1) was neutralized, filtered, washed, dried, and sieved similar to the method used for CIB. The crosslinked CIB was designated as CIB-ECH [Scheme 1(B)].

Grafting of Polyaniline Onto Chitosan Immobilized Bentonite and Crosslinked Chitosan Immobilized Bentonite. About 4 g (CIB) or (CIB-ECH) in 40 mL of 2 wt % acetic acid was combined with 40 mL 1*M* HCl containing 1 g aniline at 25°C. The solution was cooled at 5°C in an ice/water bath and stirred continuously. Then 10 mL of 1*M* HCl solution containing 0.1 g $(NH_4)_2S_2O_8$ was added. The solution was kept at 5°C for 1 h, then the bath was removed and stirring continued for 3 h. Following the reaction, the solution was neutralized (to pH $\geq$ 7) by 1*M* NaOH solution. The precipitates were filtered, washed with deionized water three times. In order to separate the PANI from the obtained precipitates, 2 wt % acetic acid was added, followed by removal of the insoluble PANI. Afterwards, 1*M* NaOH solution was added to the remaining solution and new precipitates were formed. Finally, the resulting solutions were filtered to obtain PANI-grafted-chitosan immobilized bentonite [Scheme 1(C)] and grafted-crosslinked chitosan immobilized bentonites [Scheme 1(D)] which were designated as PANI-*g*-CIB and PANI-*g*-CIB-ECH, respectively.

RESULTS AND DISCUSSION

Chemical modification open ways to various utilization of polysaccharides and afford novel types of tailored hybrid materials composed of natural polysaccharides, inorganic materials, and synthetic polymers. Graft copolymerization of synthetic, organic/inorganic composites can introduce desired properties and enlarge the field of their potential applications.

Herein, CIB composite was obtained by treatment of chitosan with bentonite in acidic medium [Scheme 1(A)].

The —OH groups at the bentonite surface interact with chitosan, through hydrogen bond between —NH_2 of chitosan and —OH of bentonite. In addition for the crosslinked CIB composite, the hydroxyl groups from ECH form hydrogen bonds with the silicate hydroxylated edge groups of bentonite and the hydroxyl groups of chitosan [Scheme 1(B)].[18] Therefore, PANI grafting of both CIB and CIB-ECH took place at retained —OH and NH_2 groups on the backbone of chitosan (biopolymer),[19] as illustrated in Scheme 1(C,D), respectively.

X-ray Diffraction

Figure 1(a) shows the XRD pattern for chitosan, bentonite, CIB, CIB-ECH, PANI-*g*-CIB, and PANI-*g*-CIB-ECH. The diffractogram for bentonite, CIB, and CIB-ECH show well-defined peak at 6.2° with high intensity. In addition, the XRD intensity of bentonite at peak $2\theta = 6.2°$ was observed to decrease on addition of chitosan and crosslinking agent. The interaction between

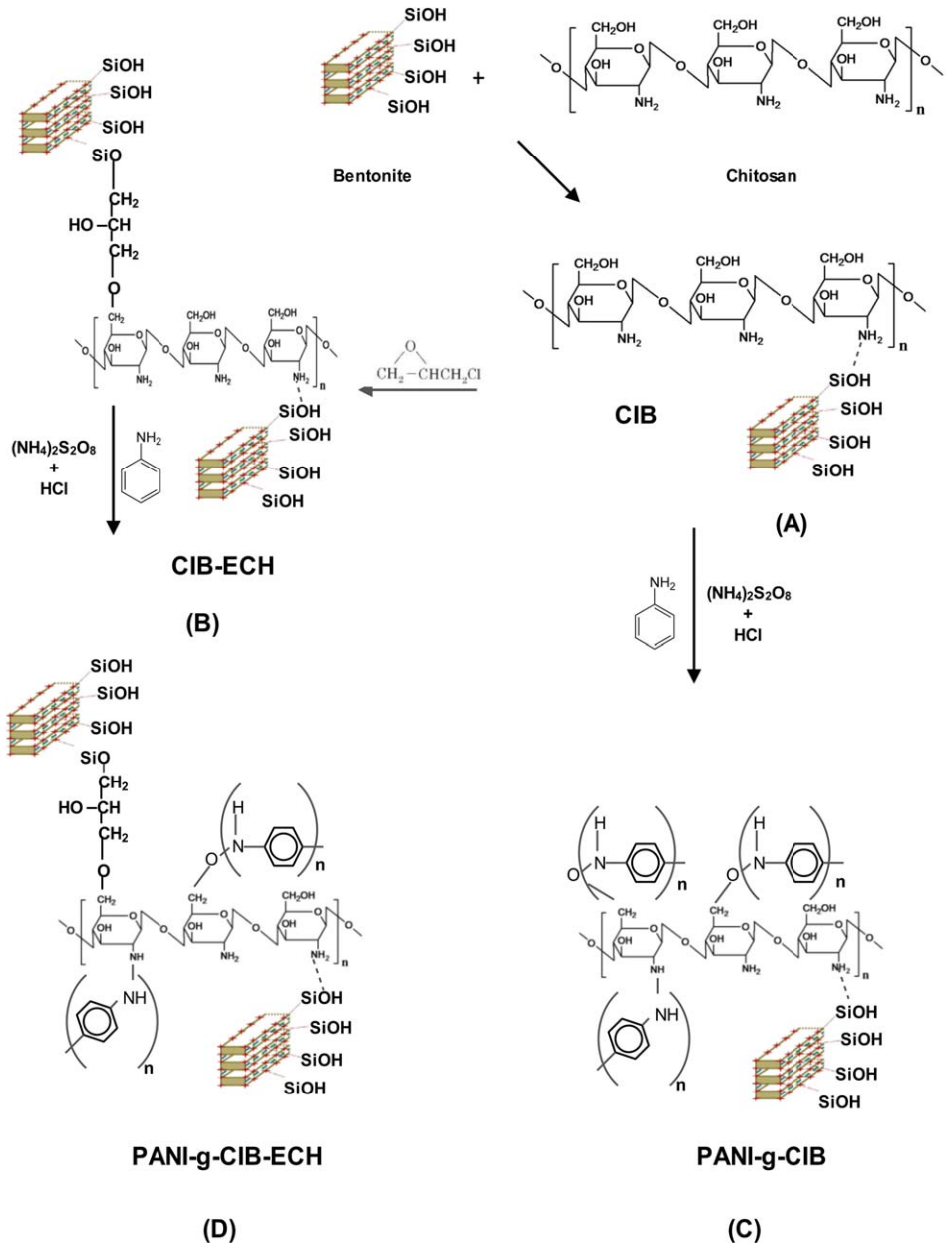

Scheme 1. Synthesis of CIB (A), CIB-ECH (B), PANI-*g*-CIB (C), and PANI-*g*-CIB-ECH (D). [Color figure can be viewed in the online issue, which is available at wileyonlinelibrary.com.]

bentonite and chitosan plus the crosslinking agent, taking into account the different molecular size and chemical structures, caused the distortion of the intrinsic lattice arrangement of bentonite, leading to a decrease in its crystallinity, which caused a decrease in peak intensity. Other characteristic 2θ peaks for bentonite were detected at 12.9°, 20.8°, and 26.6°. No significant shift in the diffraction angles of bentonite was observed on addition of chitosan and crosslinking agent (ECH) which indicates the absence of chitosan and ECH in the interlayer of bentonite.

Likewise, the main diffraction angles of CIB, CIB-ECH, and pristine PANI at $2\theta = 20.8°$ and 26.6° are retained after the graft treatment. In addition, the peak at $2\theta = 12.29°$ in the original bentonite is not shifted to small angle after addition of PANI to CIB and CIB-ECH composites. These results show that PANI is not intercalated into the interlayer space of bentonite,[21] suggesting that PANI grew onto chitosan in acidic solution and graft copolymer was produced, as shown in Scheme 1(C, D) respectively.

TGA/DSC

Figures 2 and 3 show the TGA/DSC curves of the pure chitosan, bentonite, CIB, CIB-ECH, PANI-*g*-CIB, and PANI-*g*-CIB-ECH. The TGA curve of chitosan is composed of two degradation stages. The first stage at lower temperatures (around 100°C) is originated from the loss of adsorbed water. The second region at higher temperature (220–380°C) is associated with weight

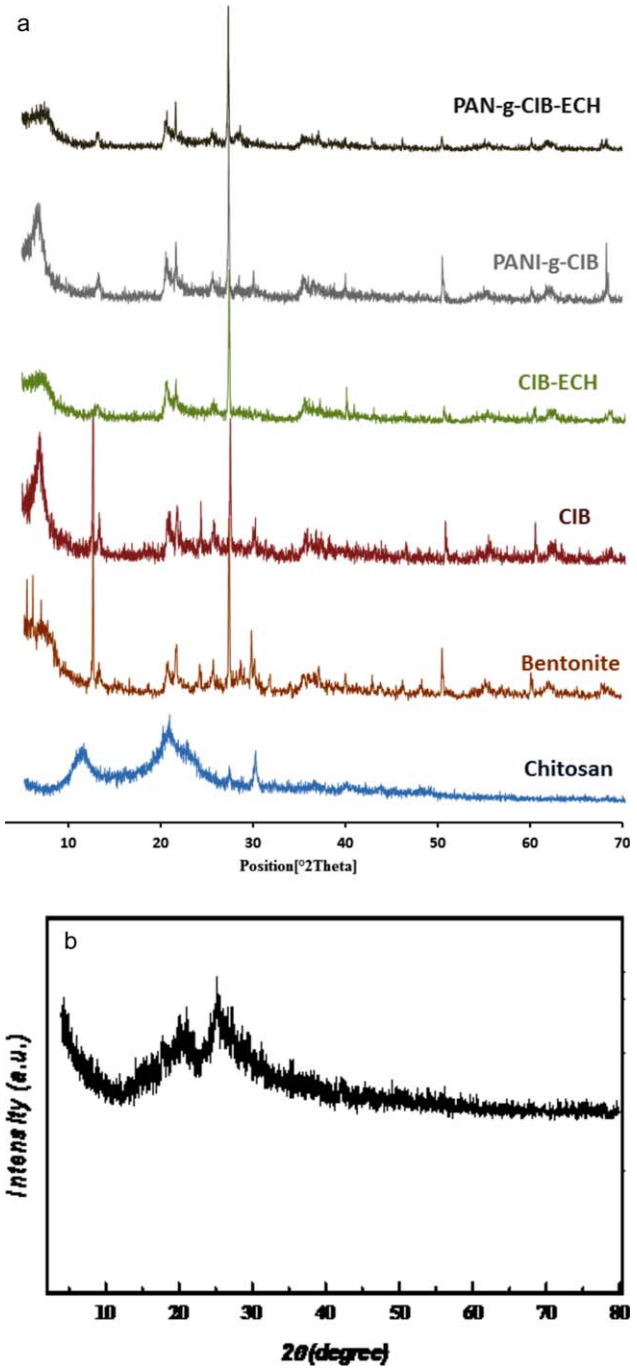

Figure 1. (a) X-ray diffractogram of chitosan, bentonite, CIB, CIB-ECH, PANI-*g*-CIB, PANI-*g*-CIB-ECH, and PANI*. (b) *X-ray diffractogram of PANI as mentioned in our previous publication.[20] [Color figure can be viewed in the online issue, which is available at wileyonlinelibrary.com.]

loss 69.96%. Chitosan was burnt out completely at 560°C. The amount of water is found to be 12%, based on the TGA weight loss data. The simultaneous TGA/DSC results show that the TGA weight loss corresponded exactly to the DSC endothermic and exothermic peaks.[22] For bentonite, the curve shows three main endothermic processes in parallel with three weight loss steps: an endothermic peak centered at 100°C is accomplished by 19.5% weight loss (TGA curve) at the temperature range

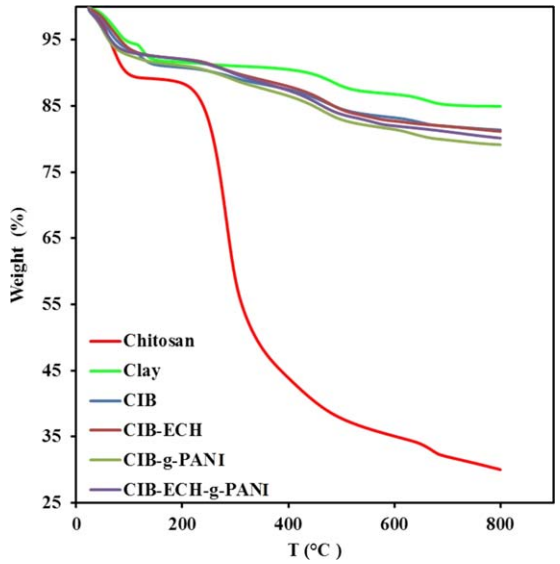

Figure 2. TGA curves of chitosan, clay, CIB, CIB-ECH, CIB-*g*-PANI, and CIB-ECH-*g*-PANI. [Color figure can be viewed in the online issue, which is available at wileyonlinelibrary.com.]

25–200°C that corresponds to the loss of physically adsorbed water on the external surface. The second endothermic peak centered at 180°C and accompanied by 6% weight loss is considered to be due to the loss of interlamellar water. A high temperature endothermic peak centered at 525°C is accompanied with 6.5%weight loss at the temperature range 400–650°C. It points to the removal of crystalline water as the silicate frame work begins to shrink and the layered structure of the montmorillonite mineral collapsed (interlayer dehydroxylation). The decomposition profile of CIB is composed of two weight loss stages, which were observed in the ranges 50–180°C and 250–700°C, the first major weight loss of 12% is due to adsorbed water. On the other, the second weight loss of 11% is composed

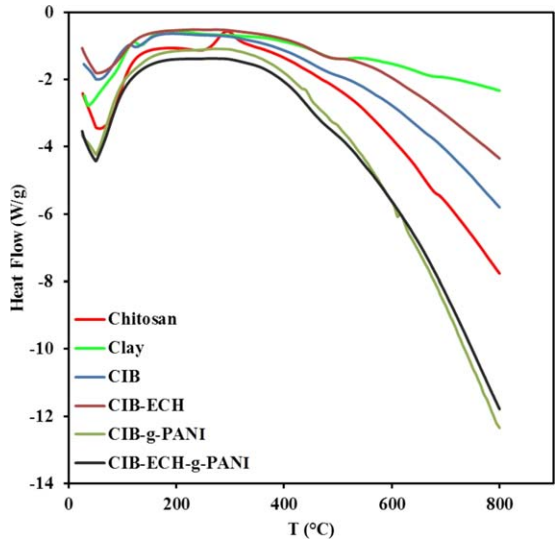

Figure 3. DSC curves of chitosan, clay, CIB, CIB-ECH, CIB-*g*-PANI, and CIB-ECH-*g*-PANI. [Color figure can be viewed in the online issue, which is available at wileyonlinelibrary.com.]

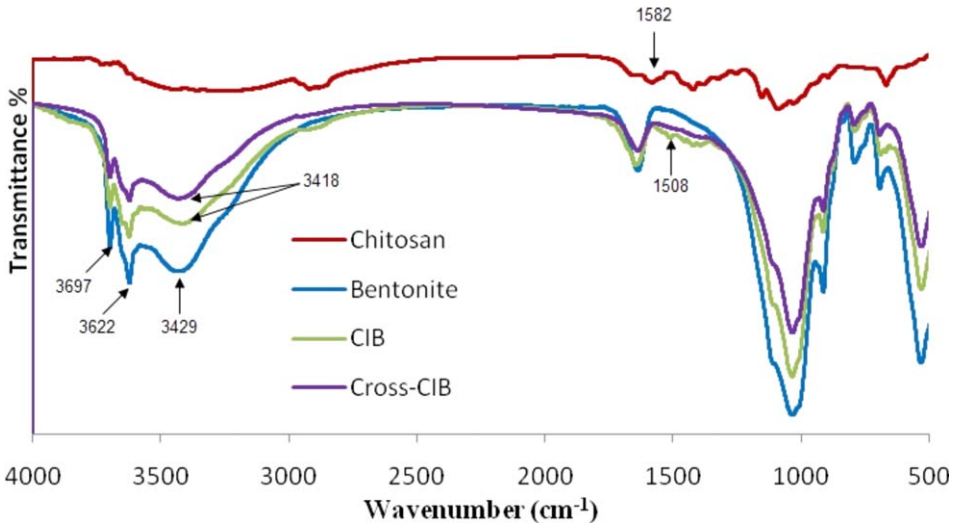

Figure 4. FTIR spectra of chitosan, bentonite, CIB, and crosslinked CIB. [Color figure can be viewed in the online issue, which is available at wileyonlinelibrary.com.]

of the decomposition of both chitosan and bentonite. Around 560°C, the chitosan would be burnt out completely from CIB, the TGA weight loss corresponds to the DSC endothermic peaks. However, for the CIB-ECH, the endothermic peak centered at 50°C is accompanied by about 10% weight loss (TGA curve) at temperature range 50–120°C, this loss can be attributed to the removal of water. At high temperature 250–700°C, the decomposition profile is similar to that of CIB and accompanied with 10% weight loss. So that TGA of CIB and CIB-ECH are more thermally stable than chitosan. The TGA studies of PANI-*g*-CIB and PANI-*g*-CIB-ECH showed that there is not much difference in the thermal behavior of these materials. Also indicates the decomposition onsets at 176°C and 18–20% weight loss up to 700°C, suggesting that thermal stability of all prepared composites could be due to the existence of inorganic clay.

FTIR

Figure 4 compares the FTIR spectra of CIB, bentonite, chitosan, and crosslinked CIB. The bands at 3697 and 3622 cm^{-1}, which are typical to hydroxyl group —OH of bentonite, located inside the sheet appeared in CIB composites with same intensity and position indicating that chitosan was not intercalated into the silicate layer. At the same time, the band at 3429 cm^{-1} which is related to OH groups on the clay surface is shifted to lower frequency 3418 cm^{-1}, suggesting interfacial interaction between chitosan and bentonite surface,[23,24] this is consistent with XRD results. However, as compared to the spectra of pristine chitosan, the frequency of vibration band at 1582 cm^{-1}, in the nanocomposite (CIB) which corresponds to the deformation vibration of protonated amine group, is shifted toward lower frequency values 1508 cm^{-1}. This shift appeared as a result of

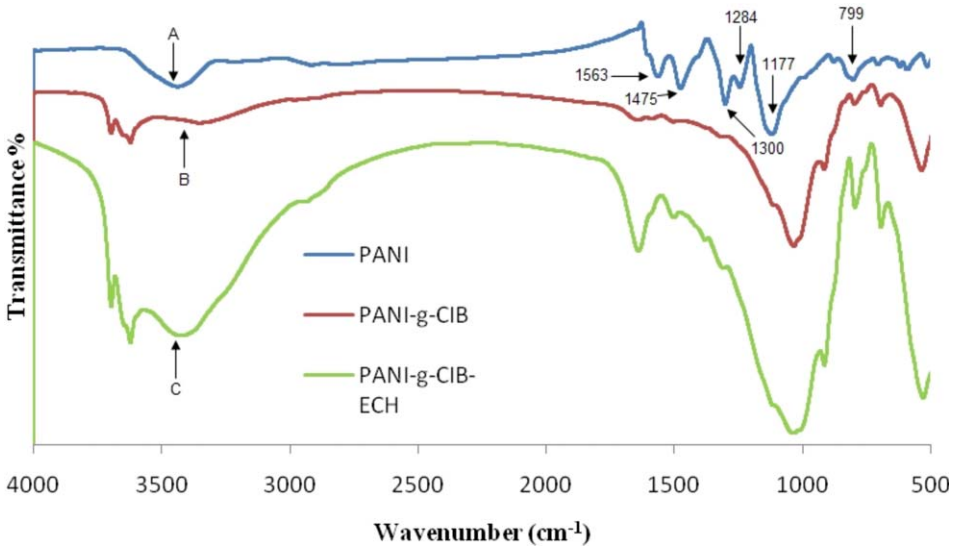

Figure 5. FTIR spectra of PANI, PANI-*g*-CIB, and PANI-*g*-CIB-ECH. [Color figure can be viewed in the online issue, which is available at wileyonlinelibrary.com.]

Table I. Electrical Conductivities of Prepared Composites with Reference to Bentonite, PANI, and Chitosan

Compound	Conductivity (S cm^{-1})
CIB	3.79×10^{-9}
CIB-ECH	4.80×10^{-9}
PANI-*g*-CIB	5.44×10^{-8}
PANI-*g*-CIB-ECH	2.32×10^{-8}
Bentonite	5.22×10^{-9}
PANI	1.5
Chitosan	9.84×10^{-16}

the electrostatic interaction between amine groups and the negatively charged sites in the clay structure, and is consistent with data in a previous report.[25,26]

The spectra of CIB-ECH showed slight changes when compared to the original CIB, because the functional groups induced by incorporating crosslinker moieties are also present in the original skeleton, so it is reasonable that no significant changes are expected for the corresponding spectra after the reaction.[27]

Figure 5 shows the FTIR spectrum of pure PANI, PANI-*g*-CIB and PANI-*g*-CIB-ECH.. FTIR spectra of composites show all significant peaks corresponding to bentonite, chitosan, and PANI. For pure PANI, the IR band at 1563 cm^{-1} corresponds to C═C stretching vibration of quinoid rings, at 1475 cm^{-1} due to C═C stretching of benzonid rings, at 1284 cm^{-1} due to C—N stretching. The absorption band 1177 cm^{-1} was assigned to N-Q-N bending.[19] The bands at 1300 cm^{-1} and 799 cm^{-1} correspond to *p*-substituted ring and aromatic C—N stretching of PANI.[28]

In PANI-*g*-CIB, the peak (B) at 3200–3500 cm^{-1} is of quite reduced intensity and broad compared to peak (A) of pure PANI, (due to overlapping of O—H stretching of chitosan and N—H stretching of aniline groups at PANI grafts). Reduced intensity of this peak with respect to chitosan shows that appreciable amounts of O—H and N—H at chitosan have been grafted with PANI.[29]

The FTIR spectrum of PANI-*g*-CIB-ECH was rather similar to that of PANI-*g*-CIB. As mentioned above, by using ECH as crosslinking agent, however with the presence of same functional groups in both ECH and chitosan, the same vibration were observed but with different relative intensities as shown in peak (C).

Electrical Conductivity Measurements

The electrical conductivity σ (Ω^{-1} cm^{-2}) was calculated from eq. (1)

$$\sigma = \frac{1}{\rho} \tag{1}$$

where ρ (Ω cm^2) is the specific resistance of materials[22] and it is calculated from eq. (2)

$$\rho = \frac{(R \times A)}{L} \tag{2}$$

where R (Ω) is the resistance, A (cm^3) is the total area, and L (cm) is the thickness of the sample.

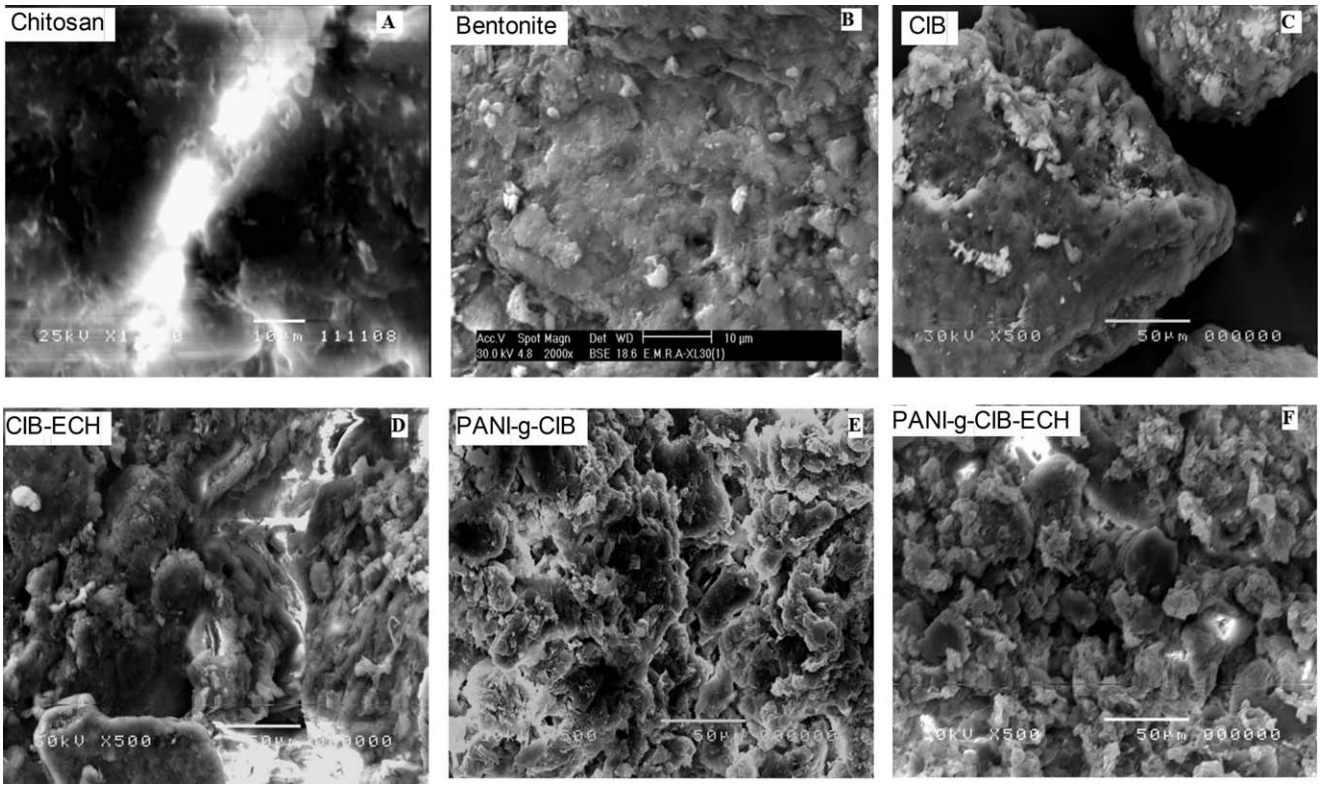

Figure 6. SEM micrograms of chitosan (A), bentonite (B), CIB (C), CIB-ECH (D), PANI-*g*-CIB (E), and PANI-*g*-CIB-ECH (F).

The electrical conductivity of all prepared samples was measured at lab condition with reference to pristine (chitosan, bentonite, and PANI). The results are summarized in the Table I. It has been clearly observed that electrical conductivity of PANI-*g*-CIB> CIB and PANI-*g*-CIB-ECH> CIB-ECH. This is attributed to grafting of PANI (pure electronic) on to chitosan backbone (insulator materials). In addition, the electrical conductivity of PANI-*g*-CIB> PANI-*g*-CIB-ECH, this may be due to the reduction in the number of sites (hydroxyl groups) on the chitosan backbone accessible for grafting after crosslinking with ECH, as illustrated in Scheme 1(D). As shown in Table I, the conductivity of PANI-*g*-CIB and PANI-*g*-CIB-ECH fall in the range required for application as ESD.

SEM

The surface morphology of all prepared samples was studied by SEM taking chitosan as reference. As shown in Figure 6(A–F), the surface of pure bentonite was flaky texture reflecting its layered structure.[26] The exterior surface of CIB showed slightly smooth surface with cotton-like accumulation of irregular shape, while surface view of chitosan shows tightly bound structure with slightly large voids, giving shape like that accumulated on surface of CIB image. By crosslinking chitosan coated with bentonite (CIB-ECH), surface image shows interlinked structure with fewer voids. PANI-*g*-CIB and PANI-*g*-CIB-ECH composites have flower petals like appearance. The micrographs of PANI-*g*-CIB composite exhibit more dense structure (high density granules per unit area) compared to PANI-*g*-CIB-ECH, less density per area. It shows that number of PANI chains in PANI-*g*-CIB>PANI-g-CIB-ECH which is consistent with electrical conductivity results.

CONCLUSIONS

Chitosan immobilized on bentonite CIB (5% chitosan) was prepared, and then the product material was crosslinked using ECH as crosslinking agent. The nanocomposites CIB and CIB-ECH were grafted with PANI using ammonium peroxydisulphate. The addition of PANI to organic/inorganic composites provides new synergistic properties that cannot be attained from individual materials. FTIR and XRD analysis suggest that chitosan was not intercalated into the silicate layer. The electrical conductivity obtained in the present study is suitable for application as ESD. The high thermal stability was evident from TGA/DSC curves. Thus we offer an alternative, simple, and economic cheap route for the preparation PANI-*g*-CIB and PANI-*g*-CIB-ECH composites with controlled conductivity.

ACKNOWLEDGMENTS

The authors would like to thank the head of the Egyptian Petroleum Research Institute (EPRI) and all members of the petrochemicals department for helping to produce this work. With grateful authors still remember the late professor Mohammed H. M. Hussein the pioneer researcher in chitosan at their institute.

REFERENCES

1. Li, Q.; Dunn, E. T.; Grandmaison, E. W.; Goosen, M. F. A. *J. Bioact. Compat. Polym.* **1992**, *7*, 370.
2. Wan Ngah, W. S.; Fatinathan, S. *Chem. Eng. J.* **2008**, *143*, 62.
3. Gecol, H.; Ergican, E.; Miakatsindila, P. J. *Colloid Interface Sci.* **2005**, *292*, 344.
4. Wan, M.-W.; Petrisor, I. G.; Lai, H.-T.; Kim, D.; Yen, T. F. *Carbohydr. Polym.* **2004**, *55*, 3, 249.
5. Bhattacharyya, K. G.; Gupta, S. S. *Adv. Colloid Interface Sci.* **2008**, *140*, 114.
6. Futalan, C. M.; Kan, C.-C.; Dalida, M. L.; Pascua, C.; Wan, M.-W. *Carbohydr. Polym.* **2011**, *83*, 697.
7. Kamari, A.; Wan Ngah, W. S. *Colloids Surf. B.* **2009**, *73*, 257.
8. Crini, G.; Badot, P.-M. *Prog. Polym. Sci.* **2008**, *33*, 399.
9. Gustafsson, G.; Cao, Y.; Treacy, G. M.; Klavetter, F.; Colaneri, N.; Heeger, A. J. *Nature* **1992**, *357*, 477.
10. Sailor, M. J.; Ginsburg, E. J.; Gorman, C. B.; Kumar, A.; Grubbs, R. H.; Lewis, N. S. *Science* **2009**, *249*, 1146.
11. Gao, F. *Mater. Today* **2004**, *7*, 50.
12. Riede, A.; Helmstedt, M.; Riede, V.; Zemek, J.; Stejskal, J. *Langmuir* **2000**, *16*, 6240.
13. Wang, H.; Li, W.; Lu, Y.; Wang, Z. *J. Appl. Polym. Sci.* **1997**, *65*, 1445.
14. Santos, M. A.; Grazina, R.; Pinto, M.; Farkas, E. *Inorg. Chim. Acta.* **2001**, *321*, 42.
15. Wan Ngah, W. S.; Teong L. C.; Hanafiah, M. A. K. M. *Carbohydr. Polym.* **2011**, *83*, 1446.
16. Hussein, M. H. M.; El-Hady, M. F.; Shehata, H. A. H.; Hegazy M. A.; Hefni, H. H. H. *J. Surfactants Deterg.* **2013**, *16*, 233.
17. Mikhail, S.; Zaki, T.; Khalil, L. *Appl. Catal. A Gen.* **2002**, *227*, 265.
18. Grisdanurak, N.; Akewaranugulsiri, S.; Futalan, C. M.; Tsai, W. C.; Kan, C. C.; Hsu, C. W.; Wan, M. W. *J. Appl. Polym. Sci.* **2012**, *125*, 132.
19. Tiwari, A.; Singh, V. *Express Polym. Lett.* **2007**, *1*, 308.
20. El Dib, F.; Sayed, W. M.; Ahmed, S.; Elkodary, M. *J. Appl. Polym. Sci.* **2012**, *124*, 3200.
21. Wang, B.; Liu, C.; Yin, Y.; Tian, X.; Yu, S.; Chen, K.; Liu, P.; Liang, B. *J. Appl. Polym. Sci.* **2013**, *130*, 1104.
22. Hussein, M. H. M.; El-Hady, M. F.; Sayed, W. M.; Hefni, H. *Polym. Sci. Ser. A* **2012**, *54*, 113.
23. Zhirong, L.; Uddin, M. A.; Zhanxue, S. *Spectrochim. Acta A Mol. Biomol. Spectrosc.* **2011**, *79*, 1013.
24. Marins, J. A.; Giulieri, F.; Soares, B. G.; Bossis, G. *Synth. Met.* **2013**, *185*, 9.
25. Marchessault, R. H.; Ravenelle, F.; Zhu, X. X. Polysaccharides for Drug Delivery and Pharmaceutical Applications; ACS Symposium Series: Washington, DC, **2006**; Vol. *934*.
26. Darder, M.; Colilla, M.; Ruiz-Hitzky, E. *Chem. Mater.* **2003**, *15*, 3774.
27. Saifuddin, N.; Dinara, S. *Adv. Nat. Appl. Sci.* **2012**, *6*, 249.
28. Mahanta, D.; Manna, U.; Madras, G.; Patil, S. *ACS Appl. Mater Interfaces* **2011**, *3*, 84.
29. Hosseini, S. H.; Simiari, J.; Farhadpour, B. *Iran Polym. J.* **2009**, *18*, 3.